Role of cellulose nanowhiskers on the flexural properties of self-reinforced polylactic acid composites

Kazi M. Zakir Hossain[a], Reda M. Felfel[a,b], Chris D. Rudd[a], Wim Thielemans[c,d*,+] and Ifty Ahmed[a*]

[a]*Division of Materials, Mechanics and Structures, Faculty of Engineering, University of Nottingham, University Park, Nottingham NG7 2RD, United Kingdom*

[b]*Physics Department, Faculty of Engineering, Mansoura University, Mansoura 35516, Egypt*

[c]*School of Chemistry, University of Nottingham, University Park, Nottingham, NG7 2RD, United Kingdom*

[d]*Process and Environmental Research Division, Faculty of Engineering, University of Nottingham, University Park, Nottingham, NG7 2RD, United Kingdom*

[+]*Current address: Renewable Materials and Nanotechnology Research Group, KU Leuven, Campus Kortrijk, Etienne Sabbelaan 53, 8500 Kortrijk, Belgium*

[*]*Corresponding authors: ifty.ahmed@nottingham.ac.uk*, *wim.thielemans@kuleuven.be*

Abstract:

Self-reinforced polylactic acid (SR PLA) composites incorporating cellulose nanowhiskers (CNWs) were produced by coating orientated PLA fibres with a polyvinyl acetate (PVAc)-CNW mixture as a binder prior to hot compaction at 95^{o}C. PLA fibres were produced with an average diameter of 11 (± 0.9) µm via a melt-drawing process at 180^{o}C. Scanning electron microscopy (SEM) images revealed that the CNWs imparted roughness to the PLA fibre surface. Cross-sectional examination of the SR PLA composites after hot-pressing confirmed that the PLA fibres had maintained their morphology. Incorporation of 8 wt% CNWs within the SR-PLA composites revealed an increase in their flexural strength (48%) and modulus (39%) compared to the control composite (flexural strength~82 MPa and modulus~3.9 GPa). In addition, whilst the control SR-PLA composite revealed quite brittle characteristics, the addition of CNWs and PVAc gave the self-reinforced composite a more ductile behaviour.

Key words: PLA fibre, self-reinforced composite, cellulose nanowhiskers, flexural properties.

Introduction

Self-reinforced composites (SRCs) have found widespread use for applications in the biomedical, construction and packaging industries [1, 2]. The concept of self-reinforced composites was first developed by Capiati and Porter [3] who demonstrated that the orientation of aligned chains within the same polymer significantly improved their initial mechanical and fracture failure properties. In this process, fibres derived from the same polymer were heated above the glass transition (T_g) temperature but below their melting temperature (T_m) and compressed to produce composite plates using high pressure where the ultimate mechanical properties of the prepared composites depend on the molecular weight of the polymer and the fraction of aligned chains within the self-reinforced composites [4, 5]. The selection of temperature, pressure and time are very important in order to maintain optimum reinforcing effect of the fibres in SRC processing [6]. Various techniques such as hot compaction [7], partial dissolution [8], cool drawing [9] and chemical modification [10] have been employed to manufacture self-reinforced composites. Several studies have reported on the successful production of SRCs using a wide variety of polymer fibres, including polyethylene (PE) [11-14], polypropylene (PP) [15, 16], polyethylene terephthalate (PET) [17], polyamides [18, 19], polylactic acid (PLA) [4, 20, 21], polyglycolic acid (PGA) [22, 23] and polymethylmethacryalate (PMMA) [24, 25].

For biomedical applications, fibres derived from biopolymers such as poly lactic acid (PLA), poly glycolic acid (PGA), and their copolymer PLGA have been the most widely investigated for SRC processing [21-23]. Amongst them, PLA is one of the most common bioresorbable polymers utilised for internal bone fixation implants due to its favourable degradation and

mechanical properties, and availability with different lactide contents (i.e. L/D ratio) [26, 27]. In order to produce SRCs with superior mechanical properties, it is desirable to develop high modulus and high strength fibres. The mechanical properties of PLA fibres have been shown to be improved with aligning/orientation of the molecular chains during fibre spinning [28] and drawing processes [29-31]. For example, Mezghani and Spruiell [28] reported increased tensile strength and modulus of as-spun Poly(L-lactic acid) (PLLA) filaments from 80 MPa to 385 MPa and from 3.7 GPa to 6 GPa respectively, by decreasing the fibre diameter from 67µm to 13µm utilising a high speed winder drum (100 $m.min^{-1}$ to 4700 $m.min^{-1}$). They suggested that the improvement of tensile properties was attributed to an increase in crystallinity from 5% to 43% as a result of strain induced chain orientation within the polymer fibres.

For self-reinforced PLA composite processing, use of highly crystalline PLA filaments also showed significantly improved interfacial bonding due to the similar chemical structure of both matrix and reinforcing elements [32]. For example, Li and Yao [33] produced 0.5 mm thick single PLA composites using amorphous PLA sheets (5% crystallinity) and crystalline PLA yarn (40% crystallinity) via a compression moulding process at 140^{o}C, and reported that the self-reinforced PLA composite containing 25 wt% unidirectional PLA yarns (consisting of 135 continuous fibres with average diameter of around 20 µm) had improved the tensile strength by 31% and modulus by 48% when compared to the control PLA sheet (tensile strength~44.8 MPa and modulus~2.5 GPa). The flexural properties of a 3.2 mm thick self-reinforced PLLA composite produced via a hot compaction process at 95^{o}C were investigated by Wright-Charlesworth *et al.* [20] and reported that SR-PLLA had higher initial flexural properties (strength~139.2 MPa and modulus~5.4 GPa) when compared to non-reinforced PLLA (strength~110.8MPa and modulus~3.9GPa).

Although SRCs have shown a higher strength and modulus compared to the non-reinforced polymer, recent studies have also focused on the enhancement of the material properties through modification of the processing techniques [7] as well as through the incorporation of fillers [34-36]. For instance, Foster *et al.* [37] investigated the incorporation of carbon nanofibres (CNF) into hot compacted polypropylene (PP) woven tapes and also the addition of other nano and micro-sized fillers, such as talc, nanoclay, fly ash and carbon black [35]. It was reported that all of the fillers improved the interlayer adhesion properties compared to the pure PP tape/film, which was confirmed via SEM images and peel testing.

Natural polymers such as chitosan [38], alginate [39] and cellulose [40, 41] both in nano and microfibre form have also been incorporated in PLA for use in tissue engineering and biomedical applications. Cellulose nanowhiskers (CNWs) have widely been investigated in nanocomposites [40-44] processing due to their biodegradability [45-47], biocompatibility [48, 49] and superior mechanical properties (tensile modulus ~105 GPa for cotton based nanocellulose) [50].

In this study, PLA fibre mats were prepared using melt-spun PLA fibres coated with a blend of cellulose nanowhiskers (CNWs) and polyvinylacetate (PVAc). Recently, we investigated the blend of CNWs and PVAc as a coating material on individual PLA fibre surfaces, which demonstrated that a PVAc/CNW blend was beneficial by imparting surface roughness as well as increasing the mechanical properties of the fibre. [51] A composition of 75 wt% CNW and 25 wt% PVAc was found to have the greatest improvements, and this blend was used in the work presented here. The attachment of nanowhiskers onto the fibre mats was examined via scanning electron microscopy (SEM). The self-reinforced composites investigated in this study were produced via a hot compression process by laminate stacking

the PLA fibre mats and the effect of CNWs and PVAc on the structural and mechanical properties of the composites are reported.

Materials and Methodology

PLA fibre drawing

PLA fibres were produced via a melt-drawing process [52]. Briefly, vacuum dried (at 50^{o}C for 48h) PLA beads (NatureWorks LLC, Ingeo^{TM} Grade 3251D, average M_w~90,000-120,000 g mol^{-1}, Density=1.24 g cm^{-3}) were melted at 180^{o}C in air using a steel mould, which was heated with a band heater, and comprising a 2 mm hole at its base. Molten polymer exited through the base of the mould via the hole under the effect of gravity and was drawn downwards and collected on a drum using traverse mode at 0.025 mm spacing and rotating at 400 m min^{-1}, which was found optimal for the production of higher strength PLA fibres (Table 1) [51, 52]. The drum had a diameter of 1 m with a collector distance of 50 cm from the steel mould.

Preparation of Cellulose Nano Whiskers (CNW)

CNWs were produced via acid hydrolysis of cotton (purchased from Fisher Scientific, UK) in aqueous H_2SO_4 (64 wt%) (Fisher Scientific, UK) for 45 min at 45^{o}C [40, 53]. The hydrolysed cotton was washed with de-ionised water followed by centrifugation at 10^{o}C (three cycles, each at 10,000 rpm for 15 minutes) and then dialysed under running tap water for 48h to ensure removal of free acid. Sonication was then carried out to homogenise the dispersion. Insufficiently hydrolysed fractions were removed by filtration using a fritted glass filter (n^{o}2 porosity grade) prior to treatment with Amberlite resin (purchased from Fisher Scientific, UK) to remove non-H_3O^+ cations. The CNW suspension (concentration ~0.2 wt% in deionised

water) was then freeze-dried after quench freezing with liquid nitrogen to obtain dried nanowhiskers.

Manufacture of PLA fibre mats

Aligned PLA fibre mats were produced by adding a coating of a 2 w/v% of CNWs/PVAc (75/25 wt%) blend in deionised water using a syringe needle followed by gently brushing to disperse the coating materials onto 10 layers of PLA fibres collected on the drum. PVAc was used as a binder to retain the integrity of aligned PLA fibres while CNWs were blended in to improve the mechanical properties of the coating. PVAc was obtained as Kollicoat SR (a 30% dispersion of PVAc, weight average M_w ~450,000, density 1.045 g cm^{-3}, viscosity ~100 mPa.s at 20^{o}C), which was stabilised with polyvinylpyrrolidone and sodium laurile sulphate. Preliminary testing indicated that the blend containing 75 wt% CNWs and 25 wt% PVAc was the most effective in enhancing the tensile properties of the PLA fibres.[51] We therefore chose to use this blend in this work. After drying at room temperature for 24 h, the fibre mat (with an average thickness of 0.4 mm) was removed from the drum and cut into 80 mm x 80 mm squares. It has to be noted that the initial coating onto the drum was performed only on the upper surface of the layers of fibres in order to produce a unidirectional fibre mat and also to facilitate easy removal of fibre mat from the collection drum without losing the alignment of PLA fibres. A final coating using the same blend was applied onto the cut portion of fibre mat by dipping the mat into the coating blend for 5 min. After dipping the mat was dried at room temperature for 24 h. To ensure consistent deposition of the coating materials onto the individual fibre mats, the coating suspension was replaced with a fresh suspension after each dip coating process. The overall coating materials incorporated after the final coating onto the fibre mats was determined to be around 8 wt% (6 wt% CNWs and 2 wt% PVAc) after drying at 37^{o}C for 48 h on a polytetrafluoroethylene (PTFE) sheet.

Self-reinforced composite processing

To prepare SR composites, 22 layers of coated fibre mats were stacked together and preheated at 95±3^{o}C for 15 min within a metal mould (dimension 80 mm x 80 mm x 1 mm) before pressing at the same temperature at 90 bar pressure for 10 min and cooling down to room temperature while retaining the applied pressure.

Characterisation

Electron microscopic analysis

The surface morphology of coated and uncoated PLA fibres and the shape of the CNWs produced in this study were characterised using scanning electron microscope (SEM) and transmission electron microscopy (TEM), respectively as described elsewhere [51]. A sputtered platinum coating (at 2.2 kV for 90s) was employed for SEM analysis to avoid image distortion due to charging (at an accelerating voltage of 10 kV and working distance of 10 mm). For TEM analysis an accelerating voltage of 80 kV was employed after staining the CNWs, deposited on a carbon grid treated with an oxygen-argon (25%-75%) plasma to render it more polar, with uranyl acetate (Sigma-Aldrich, UK) (2 wt % solution in water) for 2 min.

Optical microscopic analysis

In order to investigate the fibre structures within the SR-PLA composites produced in this study, resin embedded SR composites were polished utilising progressively finer sand papers prior to analysis of the cross section of the composites using a calibrated optical microscope (20x magnification).

Differential scanning calorimetric (DSC) analysis

DSC studies were conducted on a DSC Q10 (TA Instruments, USA) calorimeter over a temperature range from 20^{o}C to 210^{o}C at a heating rate of 10°C min^{-1} under nitrogen gas flow (50 mL min^{-1}). At least three tests were done for each material to ensure repeatability. The percentage of crystallinity was calculated from the DSC data as described in the literature [52].

Flexural properties

The flexural strength and modulus of the composites were obtained via three point bending tests using a Hounsfield Series S testing machine according to the standard BS EN ISO 14125:1998 [54]. Sample dimension of around 22mm × 10mm × 1mm, span length of 16 mm, cross head speed of 1 mm min^{-1} and a 5kN load cell were used to measure the flexural properties and the average values were obtained from at least five repeats.

Statistical analysis

Unpaired *t*-tests were conducted to investigate statistically significant differences between the means of the data sets obtained. To interpret the t-test results, a two-tailed *P*-value (*P*) was considered with a 95% confidence interval and a significance level of 0.05.

Results and Discussion

In this study CNWs were incorporated as a nanofillers at the fibre-matrix interface of SR PLA composites. PVAc was used as a binder to attach the CNWs to the PLA fibre surface. The modified fibres where then used in unidirectional fibre mats in order to investigate the effect of CNWs on the mechanical properties of the obtained SR PLA composites.

Morphological properties of PLA fibre mats and CNWs

SEM image presented in Figure 2a revealed a smooth surface morphology of the melt-spun PLA fibres with an average diameter of 11 (±0.9) µm. TEM images of the CNWs showed (seen in Figure 2b) their rod-like shapes in line with the literature [55]. These PLA fibres and CNWs, isolated from cotton, were used in the production of unidirectional fibre mats (see Figure 3).

Figure 3a shows a representative image of the coated PLA fibre mats that were collected from the winder drum. Once removed, the fibre sheets were then coated on both sides of the fibre mats utilising a dip coating method and around 8 wt% of the coating materials were incorporated onto the PLA fibre mats (shown in Figure 3b).

The surface morphology of both sides of the PLA fibre mats and single PLA fibres coated with PVAc and CNWs-PVAc are shown in Figures 4a-f, on which the coating material deposits can be seen on both sides of the fibre mats as well as on the single fibres when comparing the images to those of the uncoated PLA fibres. The SEM images obtained for the fibre mats produced with only PVAc binder suggested attachment of PVAc onto the PLA fibre surface giving the appearance of a matt finish (see Figure 4a-c). The CNW-PVAc coated PLA fibre mats showed that the CNWs were distributed to create a textured surface on the PLA fibres (as seen in Figure 4d-f). Some flakes were also observed on the fibre mats which were

believed to be due to the deposition of aggregated CNWs during the coating process. The attachment of CNW-PVAc to the PLA fibre surface was attributed to CNW-PVAc and CNW-CNW percolating interactions, where PVAc acted as a binding agent helping to attach the CNWs onto the surface of the fibres as well as to bind the unidirectional fibre mats during the drying process, as discussed recently by our group.[51]

Differential scanning calorimetric (DSC) analysis

The glass transition temperature (T_g) for the PVAc coated PLA fibre mat did not reveal a significant change ($P>0.05$) when compared to the PLA fibre (T_g~63.5^oC), while attachment of CNW-PVAc blend exhibited a slight increase ($P<0.05$) in T_g value (~65^oC) (Figure 5a, DSC thermograms). Restriction of polymer chain mobility along the interface caused by the hydrogen bonding created between the PLA fibre surface and the PVAc-CNW coating during the drying process may be the cause of this small effect [56]. No significant changes in cold crystallisation (T_{cc}~80^oC) and melting (T_m~166^oC) temperatures ($P>0.05$) were observed for coated fibre mats compared to the uncoated PLA fibres. For all investigated SR composites, the T_g and T_m values were noted to be around 71^oC and 172^oC (Figure 5b), respectively which were significantly higher ($P<0.05$) than the values for the fibre mats. The crystallinity of control SR PLA composite was calculated to be around 49% which was significantly higher ($P<0.05$) than the crystallinity of the PLA fibres (~34%) [6]. Additional crystallization may occur during partial melting of the fibres under high pressure during composite processing. Indeed, a decreasing fibre diameter as a result of the partial melting of the outer fibre regions, can be expected to induce crystallization in the thinning fibre. However, the crystallinity of SR PLA-PVAc and SR PLA-CNW composites were found to be around 45%, which was slightly lower ($P<0.05$) than the SR PLA composite. This may be due to the

presence of PVAc matrix used as a binder that helped to retain most of the PLA fibre within the SR composite, and may reduce the additional crystallization by local mixing with PVAc.

Structural analysis of self-reinforced PLA composites

The retention of the fibre structure within the SRCs can have a significant influence on its mechanical properties. Therefore, the polished cross-sections of the SRCs produced were investigated via a calibrated optical microscope. In Figure 6a-c, the cross-section of the SRCs revealed that the morphology of the PLA fibres had been maintained after consolidation into composites. However, the fibre morphology observed was not perfectly cylindrical for all the fibres. The temperature and pressure used in this study played an important role in preserving the fibre structure. We therefore used the processing parameters (95^{o}C and 90 bar pressure) showed by Wright-Charlesworth *et al.* [36] to provide the best combination of flexural strength, modulus and ductility in SR PLLA composites.

Furthermore, the fracture surfaces of the SRCs (Figure 7a-c) obtained after the flexural test also showed the retention of the PLA fibrous structure as well as pull out of some fibres along the fractured cross-section within the SRCs.

Flexural properties

The flexural properties of the SRCs are presented in Figure 8, where the flexural strength and modulus of the SR PLA-PVAc and SR PLA-CNWs composites were seen to increase when compared to the same properties of the SR PLA composite.

The control SR PLA composite had a flexural strength and modulus of 82 MPa and 3.9 GPa, respectively, which was lower than values found by Wright-Charlesworth *et al.* [36] for SR-PLLA composites (139 MPa flexural strength and 5.4 GPa modulus). However, in this study

PLA (Natureworks–3251D) resin was investigated which contained a lower amount of L-lactide compared to the PLLA resin used in the cited work [36]. In addition, the fibre processing conditions and further improvement of their initial strength could improve the flexural properties of SRCs. For SR PLA-CNW composites the flexural strength and modulus increased to 122 MPa (~48% increase) and 5.5 GPa (~39% increase) respectively, which was comparable with other studies on SR-PLLA composites [36]. This increase in mechanical properties was attributed to the mechanical interlocking made possible by the nanofillers (CNWs) deposits on the PLA fibres within the SR PLA-CNW composite, which improved the interfacial properties between the fibre and matrix [51]. Foster et al. [35] investigated nano- and micron-size particles (nanoclay, talc, carbon black) to enhance the interlayer adhesion in SRCs, which were also believed to increase the mechanical properties of the composites. Though the SR PLA-PVAc composite exhibited an increase in flexural properties (flexural strength~102 MPa and modulus~4.6 GPa) compared to the control SR PLA composite, these values were significantly lower ($P<0.05$) compared to SR PLA-CNW, which demonstrated the influence of CNW in the coating blends to enhance the mechanical properties of SR PLA composites. The increase seen in the SR PLA-PVAc composite might be due to better chain interdiffusion at the fibre-matrix interface. This may increase interfacial strength despite some level of plasticization by PVAc. It appears the interfacial strength increase is more important.

The stress-strain curve presented in Figure 9 shows the flexural behaviour of the SRCs produced in this study, where SR PLA revealed a sudden break during testing, highlighting their brittleness. The SR PLA-CNW composite on the other hand revealed less brittle properties. The SR PLA-PVAc composites exhibited quite ductile properties during the

flexural test, most likely as a result of the presence of plasticizing PVAc within the composite. Introduction of CNWs in this plasticizing layer reduces this plasticizing effect, resulting in improved mechanical properties, as seen for the sized fibres on their own.[51]

The control SR PLA showed complete breakdown of the fibres within the composites during the flexural test (see Figure 10a). The brittleness of the SR PLA was suggested to be associated with the surrounding matrix, formed by the partial melting of the fibres. While the fracture surfaces of the SR PLA-PVAc and SR PLA-CNW composites revealed that a significant portion of the aligned fibres had been preserved, even after fully bending the composites as presented in Figure 10b-c and 11b-c, which acted as the neutral axis of SR composites during the 3-point bending test. It is to be noted from the fracture images of SR PLA-PVAc and SR PLA-CNW (Figures 10b-c) that the initial crack within the SRCs started to appear at the bottom portion of the composites located at the opposite side of applied load, which was suggested to be due to the failure of fibres along their longitudinal axis under the flexural stress condition [25]. In addition, retention of a significant portion of aligned fibres during the flexural test could also attributed to the interlayer adhesion of PLA and PVAc matrix formed during the SR composite production.

This study showed that incorporation of CNWs and PVAc in SR PLA composites improved their flexural properties and imparted ductility. The enhanced mechanical properties enable the potential use of these SR PLA composite materials within packaging and biomedical fields.

Conclusion:

The influence of CNWs and PVAc on the improvement of the flexural properties of self-reinforced polylactic acid (SR-PLA) composites was investigated in this study. CNWs and PVAc coated highly oriented PLA fibre mats were used to produce SR composite via a hot compaction process maintaining the integrity of fibre within the composites. Incorporation of CNWs and PVAc within the SR composites a significant improvement in flexural properties was achieved. For example, CNWs (8 wt%) within the SR-PLA composites exhibited 48% and 39% increase in flexural strength and modulus properties compared to the control SR-PLA composite (flexural strength~82 MPa and modulus~3.9 GPa), whereas, the PVAc binder alone used within the SR composites revealed around 27% and 18% increase, respectively. The control SR PLA showed complete breakdown of fibres consolidated within the composites, whilst, the presence of CNWs and PVAc had a significant influence on ductile behaviour of the SR composites by retaining a portion of aligned fibres even after fully bending the composites, which reduced the chances of sudden failure during flexural test.

Acknowledgements

KMZH acknowledges the University of Nottingham for a Dean of Engineering scholarship whilst WT thanks EPSRC for financial support under grant EP/J015687/1.

References

[1] C. Gao, L. Yu, H. Liu, L. Chen, Progress in Polymer Science, 37 (2012) 767-780.
[2] Á. Kmetty, T. Bárány, J. Karger-Kocsis, Progress in Polymer Science, 35 (2010) 1288-1310.
[3] N. Capiati, R. Porter, Journal of Materials Science, 10 (1975) 1671-1677.
[4] P. Törmälä, T. Pohjonen, P. Rokkanen, Macromolecular Symposia, 123 (1997) 123-131.

[5] N. Ashammakhi, H. Peltoniemi, E. Waris, R. Suuronen, W. Serlo, M. Kellomaki, P. Tormala, T. Waris, Plast Reconstr Surg, 108 (2001) 167-180.
[6] P.J. Hine, I.M. Ward, R.H. Olley, D.C. Bassett, Journal of Materials Science, 28 (1993) 316-324.
[7] Hine, P. J., Olley, R. H., Ward, I. M., Composites science and technology, 68 (2008).
[8] T. Nishino, I. Matsuda, K. Hirao, Macromolecules, 37 (2004) 7683-7687.
[9] J.-Y. Kim, Y.-W. Kim, J.-G. Lee, K.-S. Cho, Journal of Materials Science, 34 (1999) 2325-2330.
[10] C. Lan, L. Yu, P. Chen, L. Chen, W. Zou, G. Simon, X. Zhang, Macromolecular Materials and Engineering, 295 (2010) 1025-1030.
[11] D. Da Silva Perez, S. Tapin-Lingua, A. Lavalette, T. Barbosa, I. Gonzalez, G. Siqueira, J. Bras, A. Dufresne, International Conference on Nanotechnology for the forest product industry, Finland, (2010).
[12] M. Deng, S.W. Shalaby, Biomaterials, 18 (1997) 645-655.
[13] E. Devaux, C. Cazé, Composites Science and Technology, 59 (1999) 879-882.
[14] P.J. Hine, A.P. Unwin, I.M. Ward, Polymer, 52 (2011) 2891-2898.
[15] P.J. Hine, I.M. Ward, N.D. Jordan, R. Olley, D.C. Bassett, Polymer, 44 (2003) 1117-1131.
[16] I.M. Ward, P.J. Hine, Polymer, 45 (2004) 1413-1427.
[17] P.J. Hine, I.M. Ward, Journal of Applied Polymer Science, 91 (2004) 2223-2233.
[18] P.J. Hine, I.M. Ward, Journal of Applied Polymer Science, 101 (2006) 991-997.
[19] N.-M. Barkoula, T. Peijs, T. Schimanski, J. Loos, Polymer Composites, 26 (2005) 114-120.
[20] D.D. Wright-Charlesworth, D.M. Miller, I. Miskioglu, J.A. King, Journal of Biomedical Materials Research Part A, 74A (2005) 388-396.
[21] A. Majola, S. Vainionpää, P. Rokkanen, H.M. Mikkola, P. Törmälä, Journal of Materials Science: Materials in Medicine, 3 (1992) 43-47.
[22] P. Törmälä, J. Vasenius, S. Vainionpää, J. Laiho, T. Pohjonen, P. Rokkanen, Journal of Biomedical Materials Research, 25 (1991) 1-22.
[23] S. Vainionpää, J. Kilpikari, J. Laiho, P. Helevirta, P. Rokkanen, P. Törmälä, Biomaterials, 8 (1987) 46-48.
[24] D.D. Wright, J.L. Gilbert, E.P. Lautenschlager, Journal of Materials Science: Materials in Medicine, 10 (1999) 503-512.
[25] D.D. Wright, E.P. Lautenschlager, J.L. Gilbert, Journal of Biomedical Materials Research, 36 (1997) 441-453.
[26] K.A. Athanasiou, C.M. Agrawal, F.A. Barber, S.S. Burkhart, Arthroscopy: The Journal of Arthroscopic & Related Surgery, 14 (1998) 726-737.
[27] E. Waris, N. Ashammakhi, O. Kaarela, T. Raatikainen, J. Vasenius, Journal of Hand Surgery (British and European Volume), 29 (2004) 590-598.
[28] K. Mezghani, J.E. Spruiell, Journal of Polymer Science Part B: Polymer Physics, 36 (1998) 1005-1012.
[29] I.-H. Kim, S. Lee, Y. Jeong, Fibers and Polymers, 10 (2009) 687-693.
[30] H. Okuzaki, I. Kubota, T. Kunugi, Journal of Polymer Science Part B: Polymer Physics, 37 (1999) 991-996.
[31] X. Yuan, A.F.T. Mak, K.W. Kwok, B.K.O. Yung, K. Yao, Journal of Applied Polymer Science, 81 (2001) 251-260.
[32] P. Törmälä, Clinical Materials, 10 (1992) 29-34.
[33] R. Li, D. Yao, Journal of Applied Polymer Science, 107 (2008) 2909-2916.
[34] R.J. Foster, P.J. Hine, I.M. Ward, Polymer, 50 (2009) 4018-4027.
[35] R.J. Foster, M.J. Bonner, I.M. Ward, Composites Science and Technology, 71 (2011) 461-465.
[36] D.D. Wright-Charlesworth, J.A. King, D.M. Miller, C.H. Lim, Journal of Biomedical Materials Research Part A, 78A (2006) 541-549.
[37] P. Hine, V. Broome, I. Ward, Polymer, 46 (2005) 10936-10944.
[38] K. Cai, K. Yao, Y. Cui, S. Lin, Z. Yang, X. Li, H. Xie, T. Qing, J. Luo, Journal of Biomedical Materials Research, 60 (2002) 398-404.

[39] H. Zhu, J. Ji, R. Lin, C. Gao, L. Feng, J. Shen, Biomaterials, 23 (2002) 3141-3148.
[40] K.M.Z. Hossain, I. Ahmed, A. Parsons, C. Scotchford, G. Walker, W. Thielemans, C. Rudd, Journal of Materials Science, 47 (2012) 2675-2686.
[41] K. Oksman, A.P. Mathew, D. Bondeson, I. Kvien, Composites Science and Technology, 66 (2006) 2776-2784.
[42] K.M.Z. Hossain, L. Jasmani, I. Ahmed, A.J. Parsons, C.A. Scotchford, W. Thielemans, C.D. Rudd, Soft Matter, 8 (2012) 12099-12110.
[43] M.J. John, R. Anandjiwala, K. Oksman, A.P. Mathew, Journal of Applied Polymer Science, (2012) n/a-n/a.
[44] D. Liu, X. Yuan, D. Bhattacharyya, Journal of Materials Science, 47 (2012) 3159-3165.
[45] W.G. Glasser, B.K. McCartney, G. Samaranayake, Biotechnology Progress, 10 (1994) 214-219.
[46] K. Kümmerer, J. Menz, T. Schubert, W. Thielemans, Chemosphere, 82 (2011) 1387-1392.
[47] C.H. Park, Y.K. Kang, S.S. Im, Journal of Applied Polymer Science, 94 (2004) 248-253.
[48] L.H. Luo, X.M. Wang, Y.F. Zhang, Y.M. Liu, P.R. Chang, Y. Wang, Y. Chen, J Biomater Sci Polym Ed, 19 (2008) 479-496.
[49] J.M. Dugan, J.E. Gough, S.J. Eichhorn, Nanomedicine, 8 (2013) 287-298.
[50] R. Rusli, S.J. Eichhorn, Applied Physics Letters, 93 (2008) 033111-033113.
[51] K.M.Z. Hossain, M.S. Hasan, D. Boyd, C.D. Rudd, I. Ahmed, W. Thielemans, Biomacromolecules, 15 (2014) 1498-1506.
[52] K.M.Z. Hossain, A.J. Parsons, C.D. Rudd, I. Ahmed, W. Thielemans, European Polymer Journal, 53 (2014) 270-281.
[53] J.F.B. Revol, H.; Giasson, J.; Marchessault, R. H.; Gray, D. G. , International Journal of Biological Macromolecules, 14 (1992) 170-172.
[54] BS_EN_ISO_14125, in: Fiber Reinforced Plastic Composites- Determination of Flexural Properties, Geneva, Switzerland, 1998.
[55] S. Eichhorn, A. Dufresne, M. Aranguren, N. Marcovich, J. Capadona, S. Rowan, C. Weder, W. Thielemans, M. Roman, S. Renneckar, W. Gindl, S. Veigel, J. Keckes, H. Yano, K. Abe, M. Nogi, A. Nakagaito, A. Mangalam, J. Simonsen, A. Benight, A. Bismarck, L. Berglund, T. Peijs, Journal of Materials Science, 45 (2010) 1-33.
[56] J.L. Keddie, R.A.L. Jones, R.A. Cory, Faraday Discussions, 98 (1994) 219-230.

List of Figures

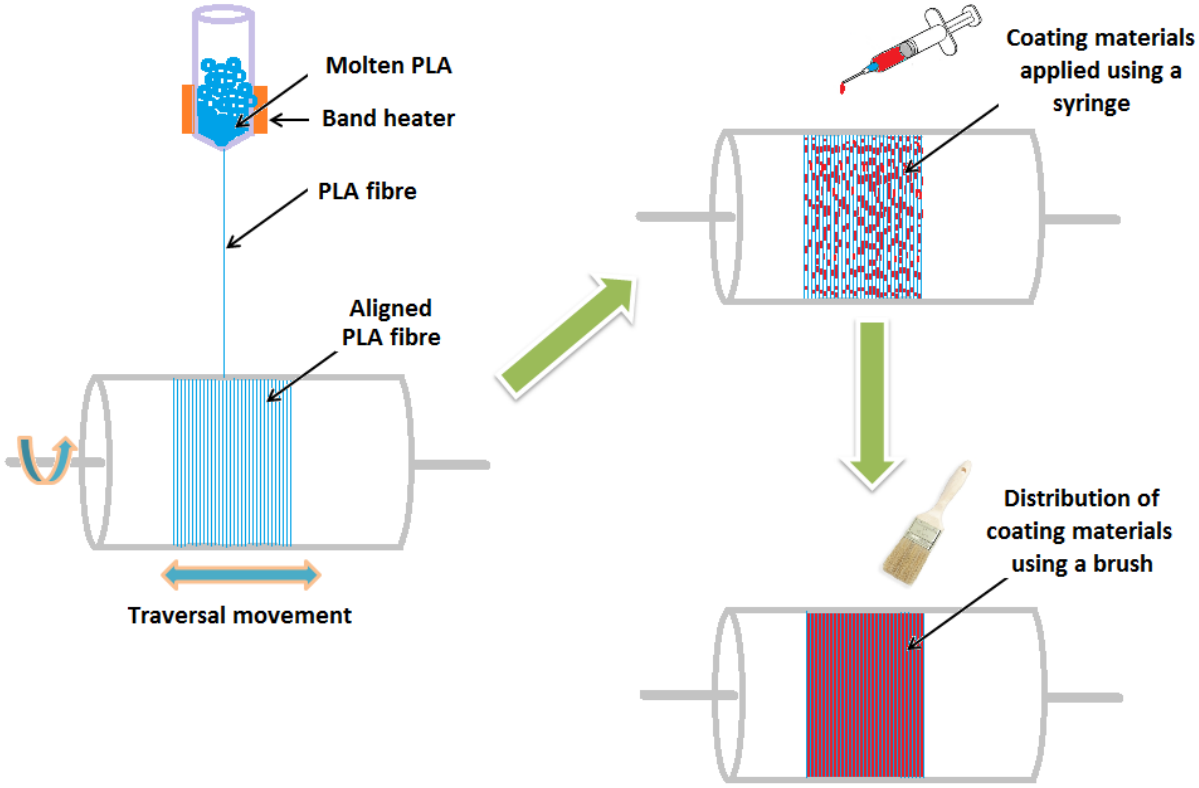

Figure 1: Schematic of PLA fibre drawing and coating procedure employed to produce aligned fibre mat.

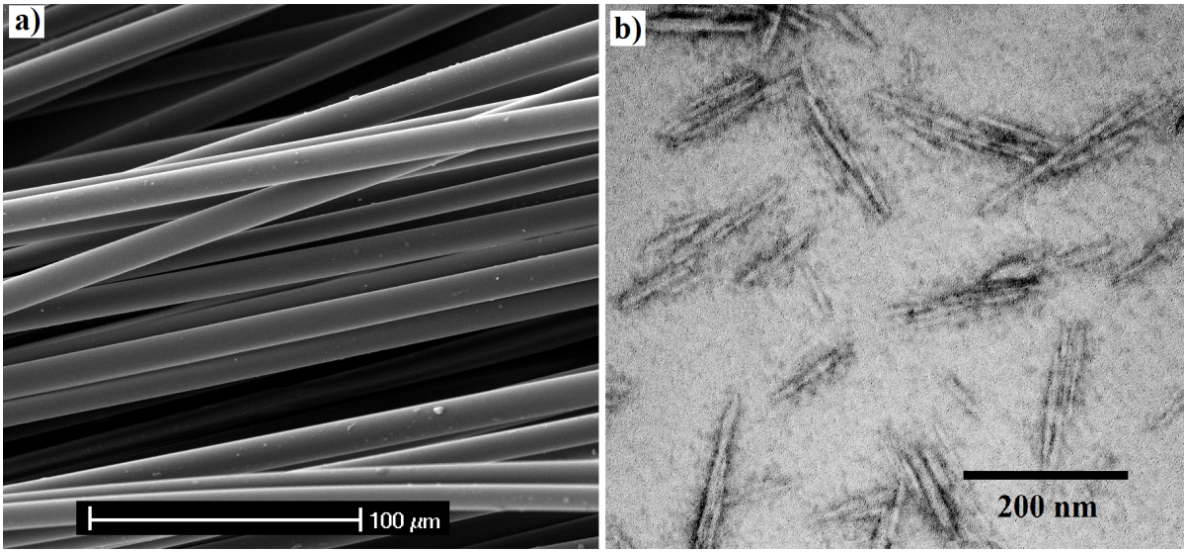

Figure 2: a) Scanning Electron microscopy (SEM) image of PLA fibres obtained at 400 m min^{-1} rotation speed, and b) TEM image of Cellulose nanowhiskers (CNWs).

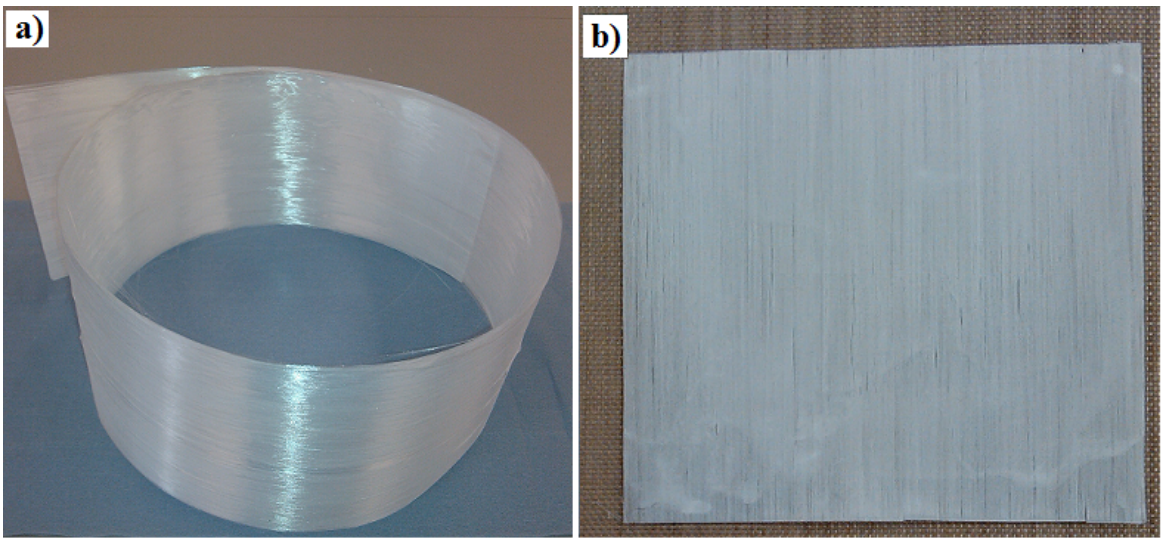

Figure 3: Representative images of PLA fibre mats a) fibre sheet collected from the winder drum after coating, and b) 80x80 mm fibre mat with both sides coated (~8 wt% coating materials).

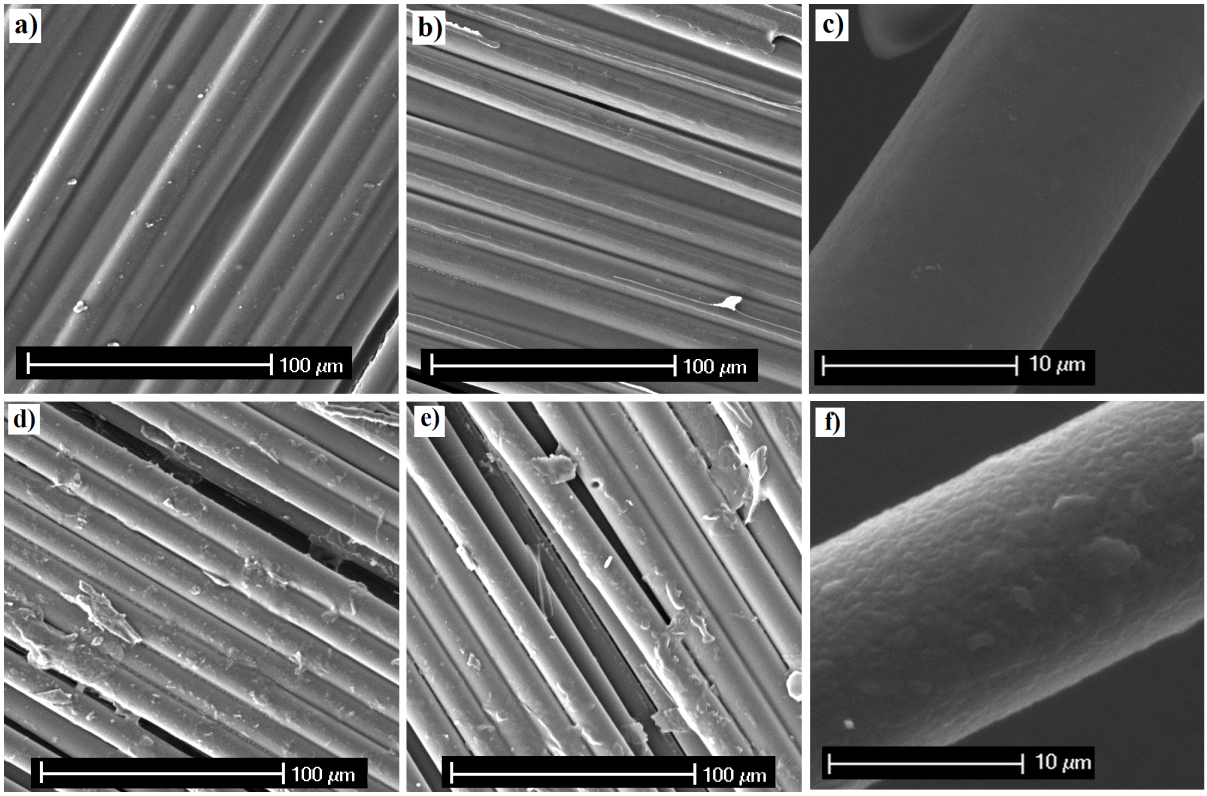

Figure 4: SEM images represent a) PVAc coated fibre mat (top surface during drying on a PTFE sheet), b) PVAc coated fibre mat (bottom surface during drying), c) PVAc coated single PLA fibre and d) CNWs-PVAc coated fibre mat (top surface), e) CNWs-PVAc coated fibre mat (bottom surface), and f) CNWs-PVAc coated single PLA fibre.

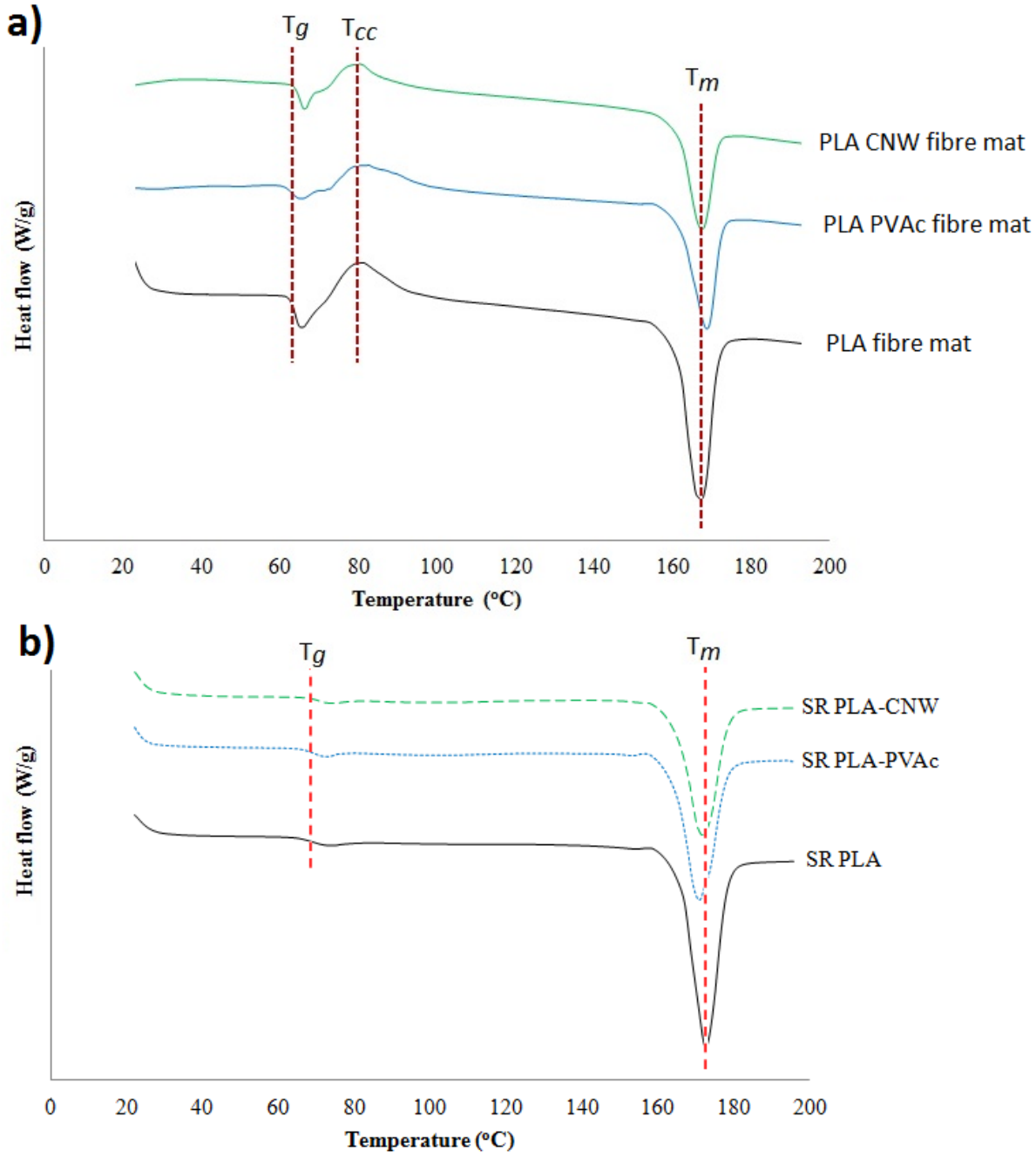

Figure 5: DSC thermogram of a) uncoated and PVAc and CNWs-PVAc coated PLA fibre mats and b) self-reinforced PLA, PLA-PVAc and PLA-CNW composites.

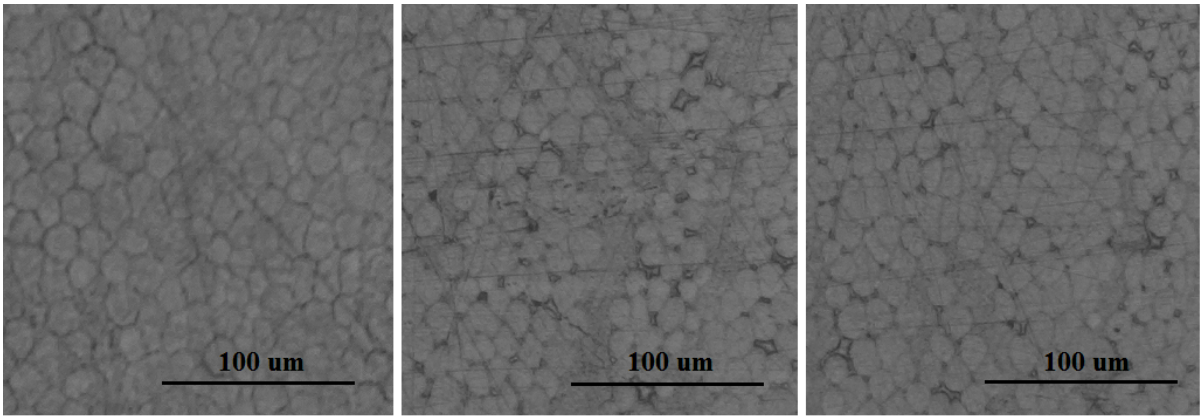

Figure 6: Optical microscopy images of polished cross-section of SR PLA composites:

a) Control (uncoated), b) PVAc coated, and c) CNWs-PVAc coated SR PLA composites.

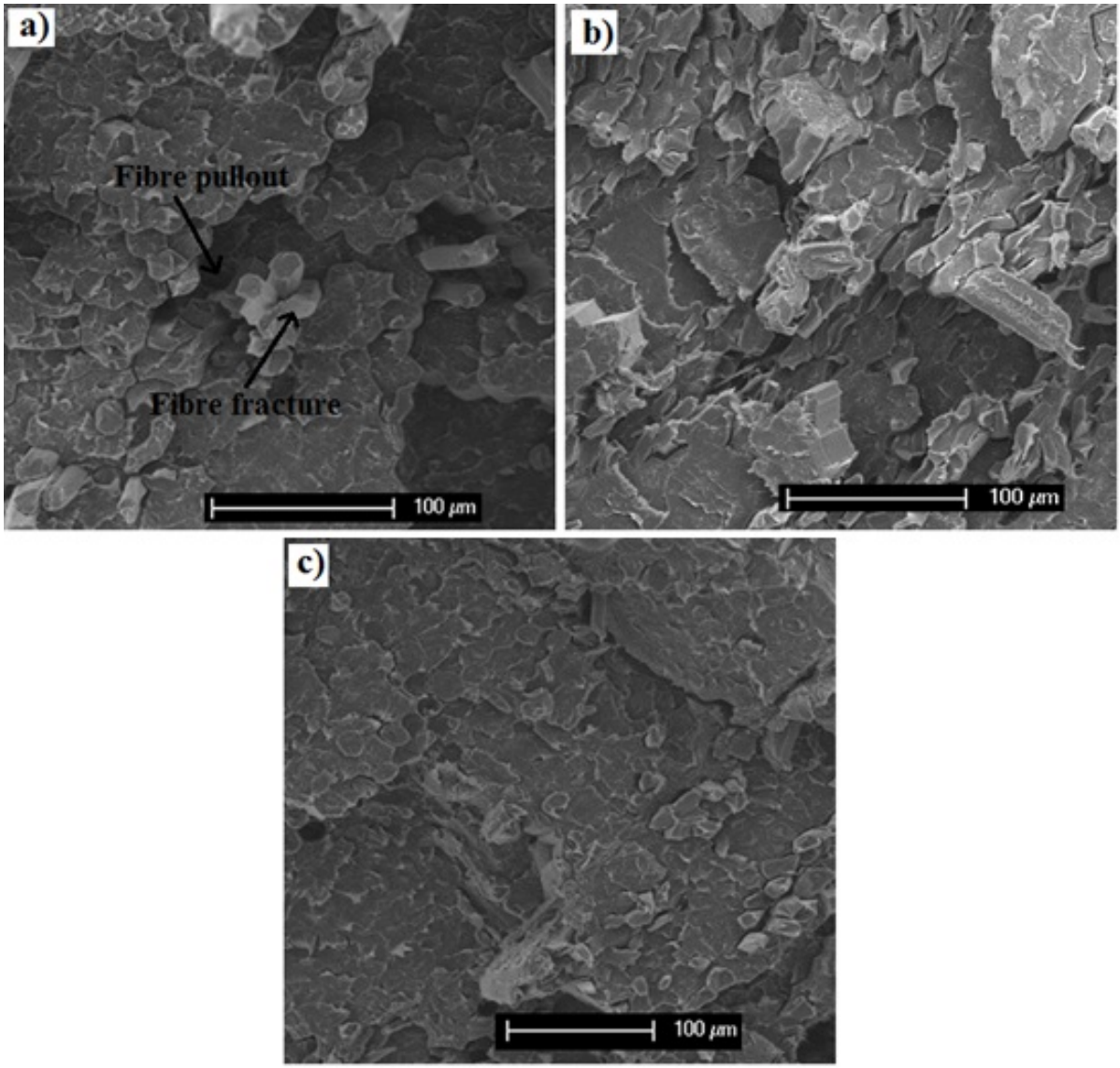

Figure 7: Scanning electron microscopy (SEM) images of fracture cross-section of SR PLA composites: a) Control (uncoated), b) PVAc coated, and c) CNWs-PVAc coated SR PLA composites

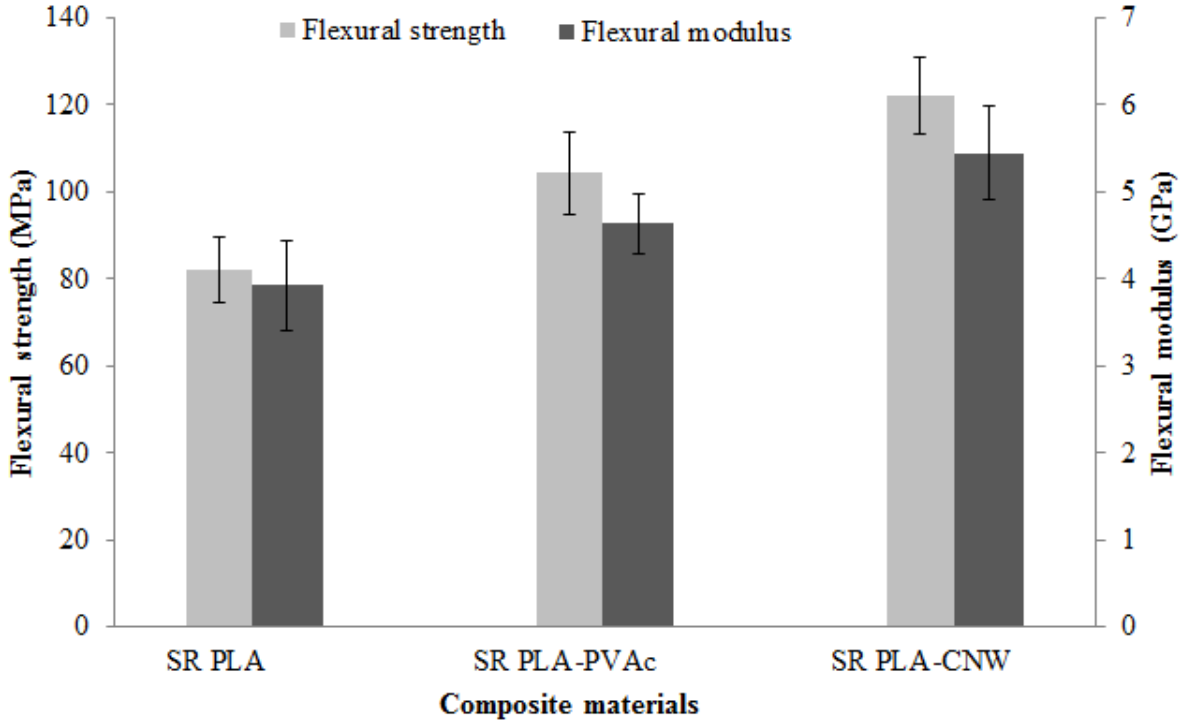

Figure 8: Flexural strength and modulus properties of self-reinforced PLA, PLA-PVAc and PLA-CNW composites produced in this study.

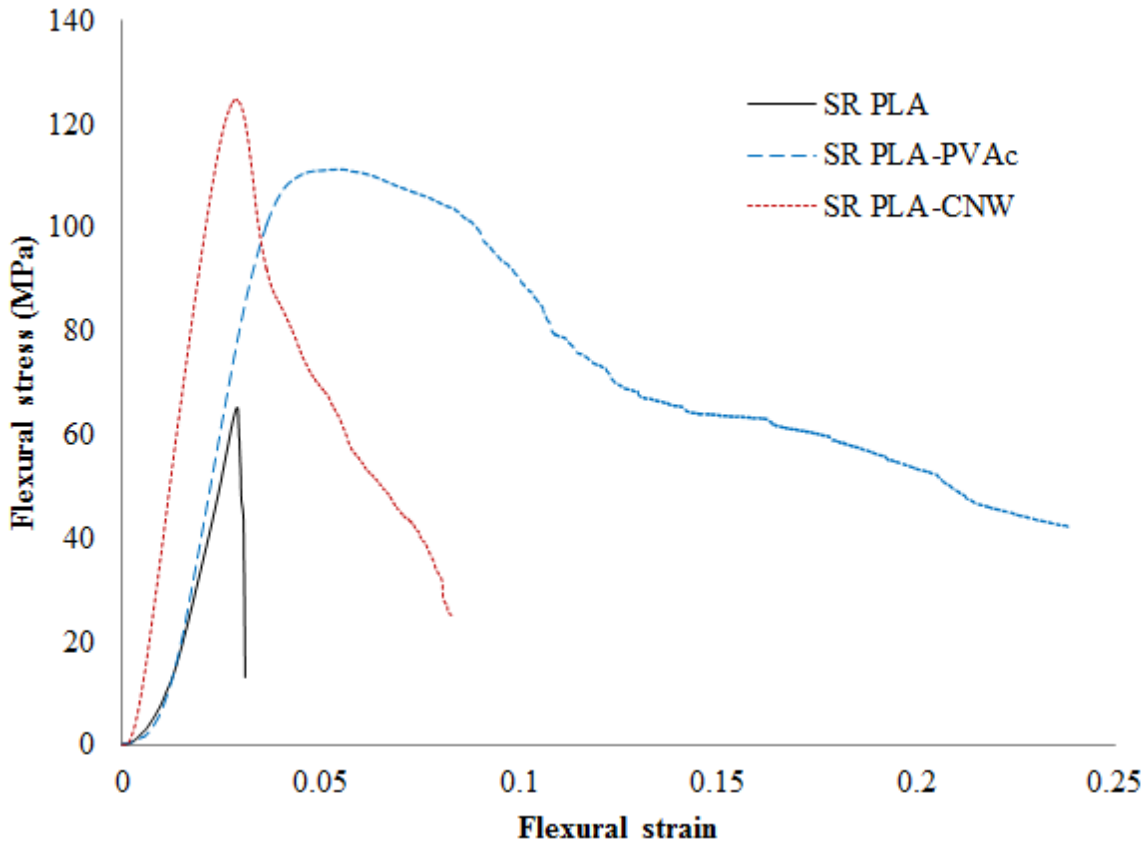

Figure 9: Typical flexural stress-strain curves for self-reinforced PLA, PLA-PVAc and PLA-CNW composites produced in this study.

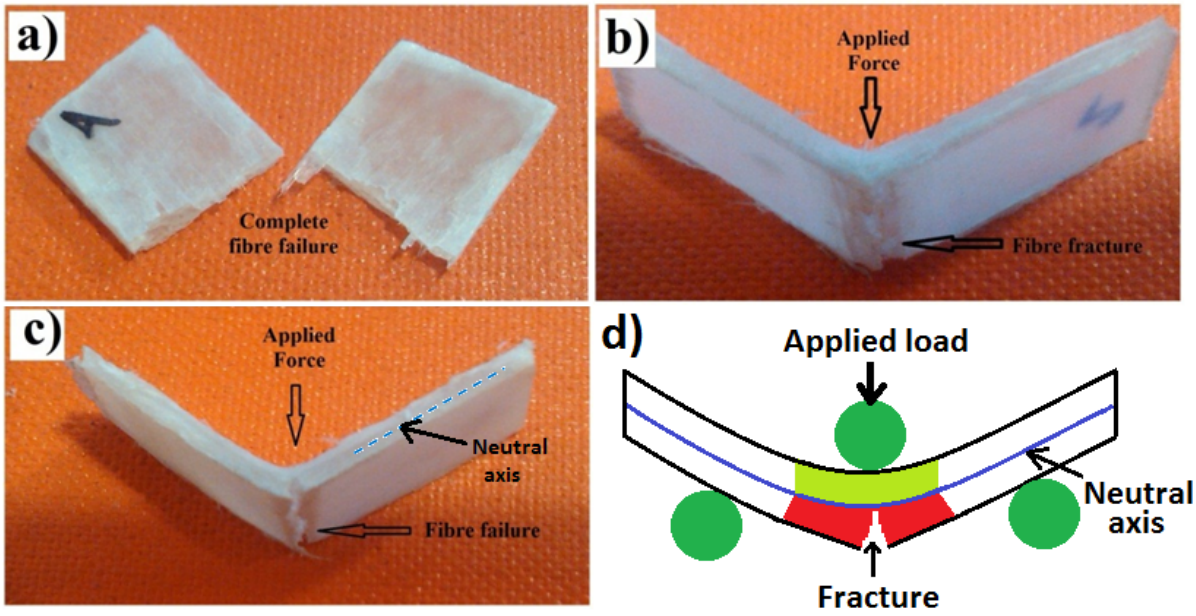

Figure 10: Image representing the fracture mode of SR composites: a) SR PLA, b) SR PLA-PVAc, c) SR PLA-CNW composite, and d) scheme of fracture mode of SR PLA-PVAc and SR PLA-CNW composites.

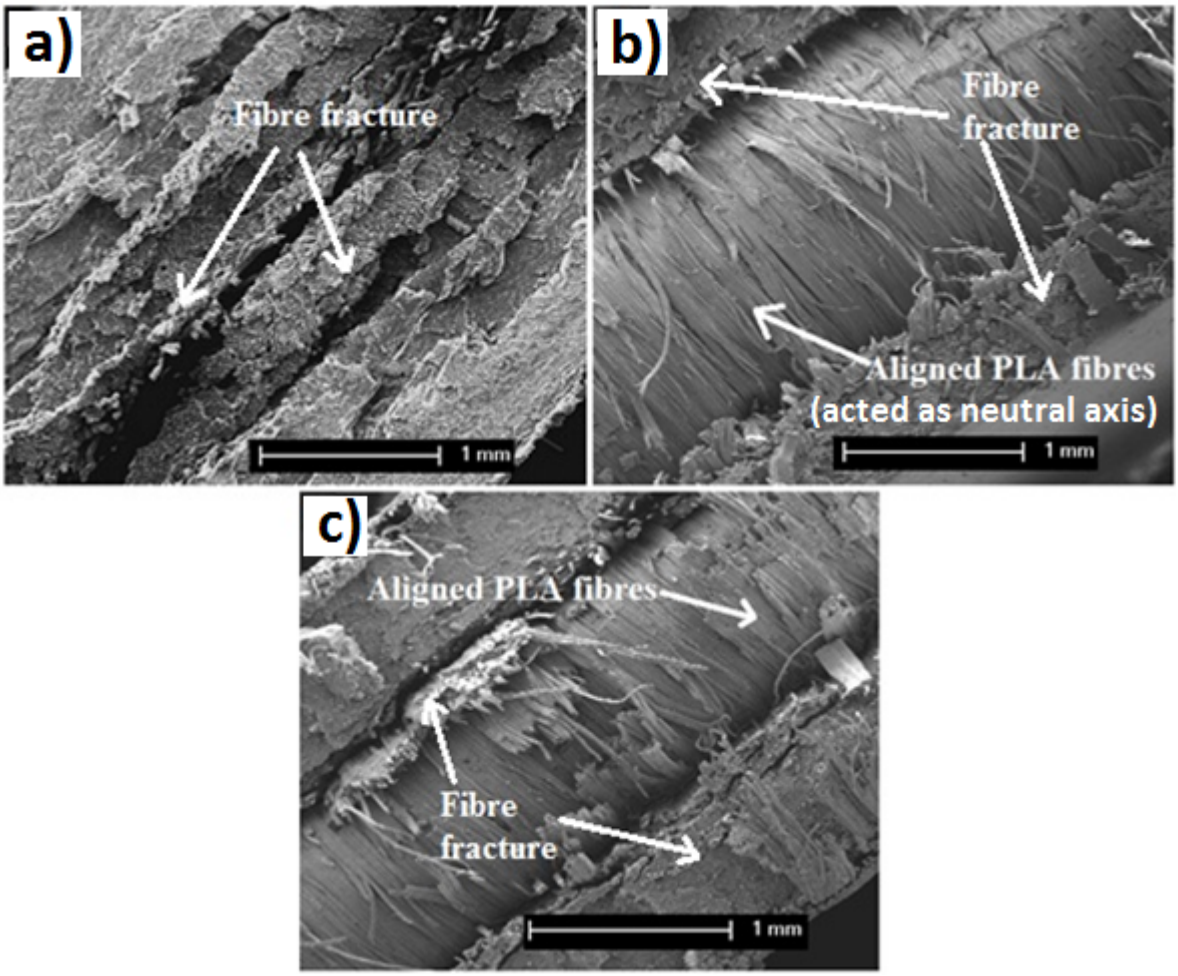

Figure 11: SEM images of the fracture surface of SRCs obtained after flexural test: a) control SR PLA (complete fracture of fibres), b) SR PLA-PVAc (partial fracture of fibres), and c) SR PLA-CNW composites (partial fracture of fibres).

List of Tables

Table 1 *Formulations of coating materials and mechanical properties of single PLA fibre coated with CNWs and PVAc.*

Sample **codes** used in this study	Coating materials		Volume fraction of PLA[a]	Tensile strength of single PLA fibre (MPa)	Tensile modulus of single PLA fibre (GPa)	References[b]
	CNWs (wt%)	PVAc (wt%)				
SR PLA	-	-	1	213 (±10) 207 (±14)	4.8 (±0.4) 4.9 (±0.3)	[1] [2]
SR PLA-PVAc	-	100	0.97	188 (±18)	5.1 (±0.1)	[2]
SR PLA- CNWs	75	25	0.93	206 (±12)	7.0 (±0.4)	[2]

[a]Volume fraction of PLA (the matrix plus the fibres) calculated on the basis of 8 wt% coating materials on fibre mat

[b]References representing the tensile properties of control and coated PLA single fibres

[1] K.M.Z. Hossain, A.J. Parsons, C.D. Rudd, I. Ahmed, W. Thielemans, European Polymer Journal, 53 (2014) 270-281.
[2] K.M.Z. Hossain, M.S. Hasan, D. Boyd, C.D. Rudd, I. Ahmed, W. Thielemans, Biomacromolecules, 15 (2014) 1498-1506.